PROCEEDINGS OF SCIENCE

Results of Nucleon Time-Like Form Factors at BESIII

Yadi Wang[a,*]

[a]*North China Electric Power University, Beinong Road No. 2, Beijing, China*

E-mail: wangyadi@ncepu.edu.cn

Precise experimental measurements of the nucleon form factors are a test-bed for understanding the nucleon's properties and dynamical behavior that emerge from QCD. With high statistics, the cross section of $e^+e^- \to p\bar{p}$ and $e^+e^- \to n\bar{n}$ are both measured with the highest precision in a wide q^2 range. An oscillation behavior is observed both on the proton and neutron effective form factors, but with an orthogonal phase difference. The electric and magnetic form factors of proton and the ratio between them are measured simultaneously with much improved precision compared with previous results through the direct annihilation method using the energy scan data from $\sqrt{s}$ = 2.0 to 3.08 GeV or through initial state radiation (ISR) method using data at $\sqrt{s}$ = 3.773 to 4.6 GeV. With the ISR technique, the form factor measurement can reach as low as the mass threshold of $p\bar{p}$ or $n\bar{n}$.

**** Particles and Nuclei International Conference - PANIC2021 ****
**** 5 - 10 September, 2021 ****
**** Online ****

*Speaker

PoS(PANIC2021)366

1. Introduction

The nucleons, proton and neutron, constituting everyday matter, have attracted great interest of physicists since last century. The electromagnetic form-factors(FFs) of the nucleon describe the structure of the nucleon as seen by an electromagnetic probe. As such, they provide a window on strong interaction dynamics over a large range of momentum [1, 2]. Moreover, they are sensitive to the gross properties of the nucleon like the charge and magnetic moment as well as the radii. In the formula of differential cross section of electron-proton elastic scattering, the electric and magnetic form factors of proton are naturally contained, see Eq.1. In recent decades, enormous theoretical progress was achieved and experimental data were accumulated concerning the space-like region for the proton.

$$\frac{d\sigma}{d\Omega_e} = (\frac{d\sigma}{d\Omega})_(Mott)\frac{E'}{E}\frac{1}{1+\tau}[G_E^2 + \frac{\tau}{\epsilon}G_E^2] \tag{1}$$
$$\tau = \frac{Q^2}{4m_p^2}, Q^2 = -q^2, \epsilon = \frac{1}{1+2(1+\tau)tan^2\frac{\theta_e}{2}}$$

In the time-like region, only a few results for form factors of proton are available, but with different trends for $R = |G_E|/|G_M|$ according to the momentum transfer q^2 [3–6]. For the form factors of the neutron, only three experiments, FENICE [7], DM2 [8] and SND [9, 10], gave results with poor precision. We report the recent results given by BESIII experiment about the form factors of proton and neutron with energy scan method and ISR method in this talk. Also we give the best precision for the cross section and effective form factors, on which an interesting oscillation is observed both for proton and neutron.

The BESIII experiment [11] is working at the $\tau-$charm factory BEPCII, which is a double-ring e^+e^- collider. The cylindrical core of the BESIII detector consists of a helium-based multi-layer drift chamber (MDC), a plastic scintillator time-of-flight system (TOF), and a CsI(Tl) electromagnetic calorimeter (EMC), which are all enclosed in a superconducting solenoidal magnet. BESIII experiment has accumulated the world's largest data sets of e^+e^- collision in the $\tau-$charm region since 2009. These provide a good opportunity for the nucleon FFs measurement.

2. Proton Form Factors

In one photon exchange case, the differential cross section of $e^+e^- \to p\bar{p}$ in the time-like region can be written as Eq. 2.

$$\frac{d\sigma}{d\cos\theta} = \frac{\pi\alpha^2\beta C}{2q^2}[|G_M|^2(1+\cos^2\theta) + \frac{4m^2}{q^2}|G_E|^2\sin^2\theta], \tag{2}$$

where $C = \frac{\pi\alpha}{\beta}\frac{1}{1-exp(-\frac{\pi\alpha}{\beta})}$ is the Coulomb factor, and m is the mass of proton. The integrated cross section is calculated with $\sigma = N^{\rm obs}/(\mathcal{L}\epsilon(1+\delta))$. $N^{\rm obs}$ is the observed number of events, $\mathcal{L}$ is the luminosity at each energy point, ϵ is the detection efficiency, and $(1+\delta)$ is the ISR correction factor. The energy scan data sets collected in the energy range between $\sqrt{s} = 2.0$ and 3.08 GeV with a total luminosity of 688.5 pb^{-1} for 22 energy points in 2015 [12] are used for the direct annihilation analysis [13].

Another merit of the ISR method is that it provides an access to the full angular distribution. Another merit with the ISR method is the full angular distribution. Thus, a better precision of the ratio $R = |G_E|/|G_M|$ is expected. Data sets of a total luminosity of 7.5 fb^{-1} collected at

$3.773 \leq \sqrt{s} \leq 4.6$ GeV are used with small angle (SA) [14] and large angle (LA) [15] ISR analyses. At event selection level, the SA-ISR event searching is performed in an untagged method, while the LA-ISR event is searched in a tagged method. The cross section with ISR method should be calculated with Eq. 3, where $W(s, x, \theta_\gamma)$ is the radiation function.

$$\frac{d\sigma_{\gamma p\bar{p}}}{dq^2 d\cos\theta_\gamma} = \frac{1}{s} W(s, x, \theta_\gamma)\sigma_{p\bar{p}}(q^2) \tag{3}$$
$$W(s, x, \theta_\gamma) = \frac{\alpha}{\pi x}\left(\frac{2 - 2x + x^2}{sin^2\theta_\gamma} - \frac{x^2}{2}\right)$$

With the large statistics of scan data in direct annihilation method, the most precise measurement of the cross sections of $e^+e^- \to p\bar{p}$ is obtained, as shown in Fig. 1 (a). The relative precision in cross section has been improved to 3% at $\sqrt{s} = 2.125$ GeV, and about 10% at other points. The effective form factor is calculated and shown in Fig. 1 (b), from which an interesting oscillation behavior is clearly observed, which shows up in the BaBar data [4, 16]. The oscillation structure can be reproduced by a dominant three-pole function (G_{3p}) and a damped oscillatory component (G_{osc}) [17]:

$$\begin{aligned} |G_{eff}| &= G_{3p} + G_{osc} \\ &= \frac{G_0}{(1 + q^2/m_a^2)(1 - q^2/0.71)^2} + Ae^{-Bp}cos(Cp + D), \end{aligned} \tag{4}$$

where $p = \sqrt{q^2(\tau - 1)}$ is the relative momentum of the proton in the rest frame of antiproton. The fit plot is shown in Fig. 1 (c). The few percent oscillation with an underlying smooth dipole-like behavior may suggest a small perturbation caused by the final state re-scattering. Other explanations from some resonant structures cannot be excluded with current results [18].

The three methods give consistent results and improve the precision in $R = |G_M|/|G_E|$ to 3.5% at $\sqrt{s} = 2.125$ GeV, shown in Fig. 1 (d), confirming the trend of BaBar data. The electric and magnetic form factors are separately extracted and shown in Fig. 1 (e) ($|G_E|$) and (f) (G_M). Benefiting from the high statistics of direct annihilation process, the $|G_E|$ is measured for the first time and with high precision. From the LA-ISR analysis, we access the mass threshold of $p\bar{p}$ for the measurement of cross section and form factors. But currently, the result is limited by low statistics.

3. Neutron Form Factors

Due to the low detection efficiency, the neutron form factors are measured only in direct annihilation method. The differential cross section of $e^+e^- \to n\bar{n}$ can also be written as in Eq. 2, but the Coulomb factor C equals to one for neutrons. The final state of $e^+e^- \to n\bar{n}$ is purely neutral, thus it is hard to detect, and the neutron can be mis-identified as photon with large probability.

Using the data collected at 18 energy values between $\sqrt{s} = 2.0$ and 3.08 GeV, the direct annihilation events of $e^+e^- \to n\bar{n}$ are selected [19]. The analysis combined three independent event classifications based on the combined information from EMC and TOF. Data-driven methods are applied to determine the efficiencies by taking into account the simulation challenges of hadronic interaction with the detector materials.

The measured Born cross section (σ_B) and the neutron effective form factor $|G_{eff}|$ are shown in Fig. 2 (a) and (b). The precision of σ_B and $|G_{eff}|$ are much improved. At $\sqrt{s} = 2.125$ GeV, the statistical uncertainty reaches 4.15%. The result given by BESIII above 2 GeV is systematically

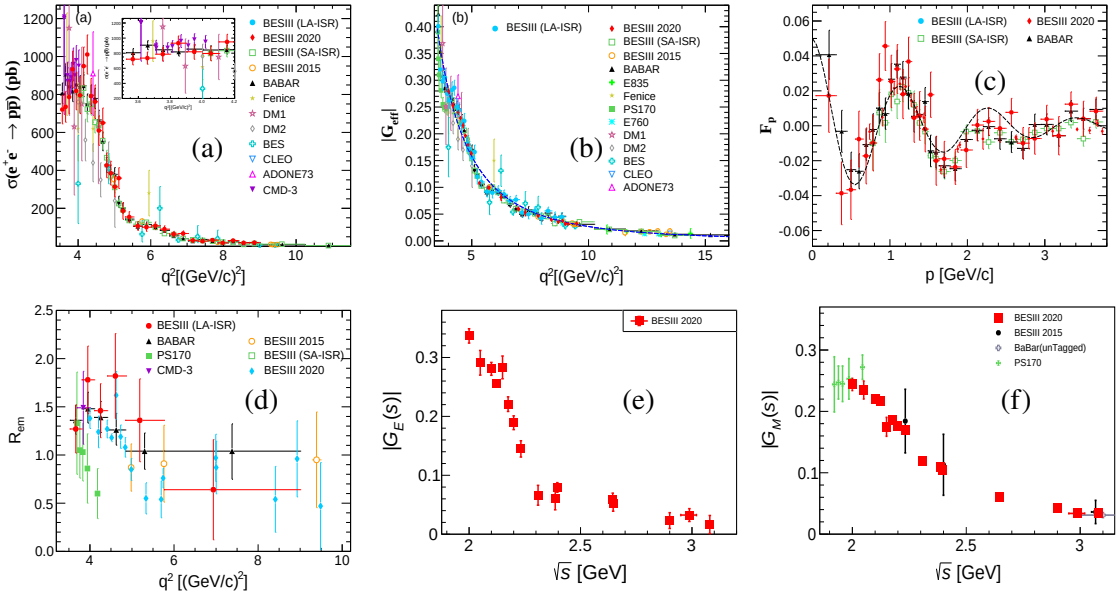

Figure 1: The cross section of $e^+e^- \to p\bar{p}$ (a), the effective form factors (b), the residual effective form factor F_p (c), the ratio between form factors $R = |G_M|/|G_E|$ (d), the electro form factor $|G_E|$ (e) and the magnetic form factor $|G_M|$ (f) compared with other experimental results. The black dots are from direct annihilation method [13]. The green boxes are from SA-ISR method [14] and the red dots are from LA-ISR method [15].

lower than all other previous experimental results, while still in agreement within 2 standard deviations. The ratio between the cross sections of $e^+e^- \to p\bar{p}$ and $e^+e^- \to n\bar{n}$ is inconsistent with FENICE result, and range from 0.25 to 1, shown in Fig. 2 (c). This result supports the predictions of stronger coupling of the virtual photon with proton than with neutron [20], and clarifies the photon-nucleon interaction puzzle which has persisted for over 20 years.

Very interestingly, the effective form factor of neutron shows also an oscillating behavior. The residual $G_{osc}(q^2) = |G| - G_D$, $G_D = A_n/(1 - \frac{q^2}{0.71(GeV^2)})^2$ is shown in Fig. 2 (d). The parameter $A_n = 4.87 \pm 0.09$ is calculated with BaBar result. The periodic structure $G_{osc}(q^2)$ is parameterized similarly as for $e^+e^- \to p\bar{p}$, but with a relative phase of $\Delta D = (125 \pm 12)°$. This result will provide theorists with much information on the nucleon structure and QCD.

4. Summary

With large statistics, BESIII experiment offers various methods and excellent platform to explore the nucleon structure knowledge and the ratio between in the time-like region. Using the energy scan data between $\sqrt{s} = 2.0$ and 3.08 GeV, the most precise measurement of the Born cross sections as well as the effective form factor of proton and neutron are extracted, which significantly improve the situation on the nucleon structure. The individual electric and magnetic form factors or the ratio between them is extracted simultaneously with very high precision in a wide q^2-range. A periodic behavior on the effective form factor of both proton and neutron is observed, which may open a new insight on the nucleon interaction. Furthermore, the physics at the threshold of $p\bar{p}$ and $n\bar{n}$ production may be studied by the ISR technique with large data sets.

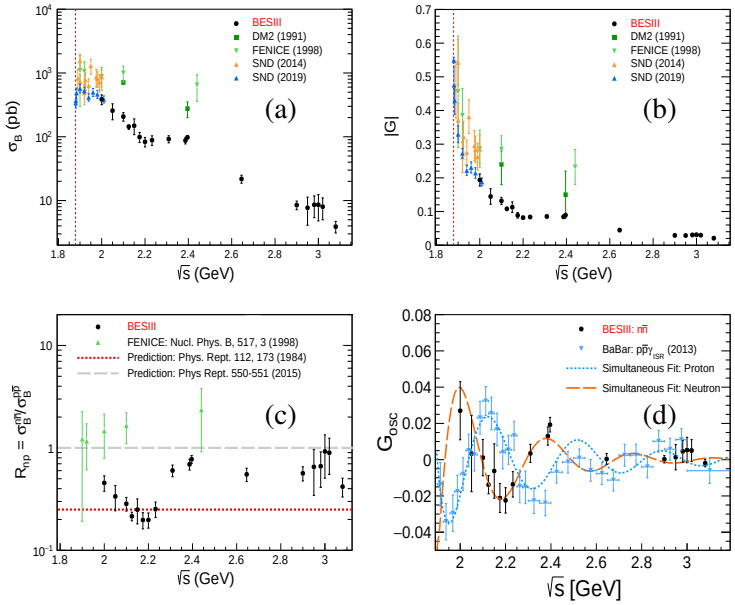

Figure 2: The cross section of $e^+e^- \to n\bar{n}$ (a), the effective form factors (b), the ratio between Born cross section of $e^+e^- \to p\bar{p}$ and $e^+e^- \to n\bar{n}$ (R_{np}) (c) and the residual effective form factor $G_{osc}(q^2)$ (d) compared with other experimental results.

References

[1] A. Denig and G. Salme, Prog. Part. Nucl. Phys. 68 (2013) 113-157.

[2] V. Punjabi, C. F. Perdrisat, M. K. Jones, E. J. Brash and C. E. Carlson, Eur. Phys. J. A 51 (2015) 79.

[3] J. P. Lees et al. (BABAR Collaboration), Phys. Rev. D 73 (2006) 012005.

[4] J. P. Lees et al. (BABAR Collaboration), Phys. Rev. D 87 (2013) 092005.

[5] J. P. Lees et al. (BABAR Collaboration), Phys. Rev. D 88 (2013) 072009.

[6] G. Bardin et al. (PS170 Collaboration), Nucl. Phys. B411 (1994) 3.

[7] A. Antonelli et al. (FENICE Collaboration), Nucl. Phys. B 517 (1998) 3.

[8] D. Bisello et al. (DM2 Collaboration), Z. Phys. C 48 (1990) 23.

[9] M. N. Achasov et al., Phys. Rev. D 90 (2014) 112007.

[10] V. P. Druzhinin and S. I. Serednyakov, EPJ Web Conf. 212. (2019) 07007.

[11] M. Abilikim et al. (BESIII Collaboration), Nucl. Instr. Meth. A 614 (2010) 345.

[12] M. Ablikim et al. (BESIII Collaboration), Chin. Phys. C 41, 063001 (2017); 41, 113001 (2017).

[13] M. Abilikim et al. (BESIII Collaboration), Phys. Rev. Lett. 124 (2020) 042001.

[14] M. Abilikim et al. (BESIII Collaboration), Phys. Rev. D 99 (2019) 092002.

[15] M. Abilikim et al. (BESIII Collaboration), Phys. Lett. B 817 (2021) 136328.

[16] A. Bianconi and E. Tomasi-Gustafsson, Phys. Rev. Lett. 114 (2015) 232301; Phys. Rev. C 93 (2016) 035201.

[17] E. Tomasi-Gustafsson, Andrea Bianconi and Simone Pacetti, Phys. Rev. C 103 (2021) 035203.

[18] I. T. Lorenz, F. W. Hammer and U. G. Meiner, Phys. Rev. D 92 (2015) 034018.

[19] M. Abilikim et al. (BESIII Collaboration), arXiv:2103.12486.

[20] V. L. Chernyak, A. R. Zhitnitsky, Phys. Rept. 112 (1984) 173.